

The Zoo of X-ray sources in the Galactic Center Region: Observations with *BeppoSAX*

L.Sidoli^{1,2}, S.Mereghetti¹, G.L.Israel^{3,4}, L.Chiappetti¹, A.Treves⁵ and M.Orlandini⁶

Received _____; accepted _____

¹Istituto di Fisica Cosmica “G.Occhialini”, C.N.R., via Bassini 15, 20133 Milano, Italy.

²Università di Milano, Sez. Astrofisica, via Celoria 16, 20133 Milano, Italy.

³Osservatorio Astronomico di Roma, Via Frascati 33, Monteporzio Catone, Roma, Italy.

⁴Affiliated to I.C.R.A.

⁵Università degli Studi dell’Insubria, Polo di Como, Dipartimento di Scienze Chimiche, Fisiche e Matematiche, Via Lucini 3, 22100, Como, Italy.

⁶TeSRE, via Gobetti 101, 40129 Bologna, Italy.

ABSTRACT

We report the results of a survey of the Galactic Center region ($|l| < 2^\circ$, $|b| < 0.5^\circ$) performed with the *BeppoSAX* satellite. The flux from the center of our Galaxy corresponds to a luminosity of $\sim 3 \cdot 10^{35}$ erg s $^{-1}$ in the 2–10 keV range. Due to the limited angular resolution ($\gtrsim 1'$) only part of it is supposed to come from Sagittarius A*, the non-thermal radio source which is believed to mark the dynamical center of the Galaxy. In addition to the diffuse emission, several bright ($L_X \gtrsim 10^{36}$ ergs s $^{-1}$) point sources have been observed, both persistent (A 1742–294, SLX 1744–299, SLX 1744–300, 1E 1743.1–2843, 1E 1740.7–2942) and transient (XTE J1748–288, SAX J1747.0–2853 and KS 1741–293).

The Low Mass X-ray Binary AX J1745.6–2901, discovered with ASCA at only 1.3' from SgrA* was detected in a low luminosity state in August 1997.

The 1–150 keV spectrum of the hard X-ray source 1E 1740.7–2942 is well described by a Comptonization model, typical of black hole candidates in their low/hard state, with no evidence for strong Fe lines.

The detection of a type I burst shows that the transient source SAX J1747.0–2853 (probably the same as the 1976 transient GX 0.2–0.2) is a LMXRB containing a neutron star.

The transient black hole candidate XTE J1748–288 was detected at a luminosity ($\sim 10^{36}$ ergs s $^{-1}$) consistent with the extrapolation of the exponential decay of the outburst observed with the XTE All Sky Monitor.

Two fainter sources are very likely associated with young neutron stars: the (possibly diffuse) X-ray source at the center of the composite supernova remnant G0.9+0.1, and the “head” of the axially symmetric radio source G359.23–0.92. The latter has been detected above ~ 6 keV, supporting a non-thermal emission mechanism.

Subject headings: Galaxy: center — X-rays: individual (A 1742–294, AX J1745.6–2901, SLX 1744–299, SLX 1744–300, 1E 1743.1–2843, 1E 1740.7–2942, XTE J1748–288, SAX J1747.0–2853, KS 1741–293, GX 0.2–0.2, G0.9+0.1, G359.23–0.92)

1. Introduction

The Galactic Center (hereafter GC) region has been observed at different spatial scales and energy bands by many X-ray missions.

The main results in the 0.5–10 keV range have been obtained with the Einstein Observatory (Watson et al., 1981), ROSAT (Predehl & Trumper, 1994) and, more recently, with ASCA (Maeda et al. 1996, 1998; Koyama et al. 1996). At higher energies, the telescopes ART-P (Pavlinsky, Grebenev & Sunyaev 1994) and SIGMA (Goldwurm et al. 1994) on-board the GRANAT satellite performed a monitoring of the GC region leading to the discovery of many new sources. These observations have shown that the GC X-ray emission comes both from point sources and from a diffuse component. Within a few degrees from the direction of the GC region there is a strong concentration of X-ray sources. The zoo of these objects is very rich and comprises both transient and permanent sources, both “standard” and very peculiar objects, like e.g. the “bursting pulsar” GRO J1744–28 (Lewin et al. 1996), the “microquasar” 1E 1740.7–2942 (Mirabel et al. 1992), and the 2 ms pulsar SAX J1808.4–3658 (in’t Zand et al. 1998a, Wijnands & van der Klis 1998).

The region ($|l| < 2^\circ$) \times ($|b| < 0.5^\circ$) around the GC was observed with the *BeppoSAX* satellite during 1996–1998 for a total of \sim 140 hours of effective exposure time (Sidoli et al., 1998a, 1999).

In this paper we report on the observations of the X-ray point sources in the GC region obtained with the *BeppoSAX* Narrow Field Instruments (for the *BeppoSAX* Wide Field Camera results see, e.g., Ubertini et al. (1999)). Although our observations cannot equal the spatial resolution obtained with ROSAT at lower energies, they provide good images with adequate spectral resolution above a few keV. The sensitivity is similar to that obtained with ASCA, that thanks to its solid state detectors has a higher spectral resolution. On the other hand, the BeppoSAX mirrors provide a narrower and more regular point response

function with respect to that of the ASCA telescopes. This allows an accurate analysis of the spatial morphology of this complex sky region and reduces the problem of stray light contamination from strong sources outside the field of view. The detailed results on the X-ray diffuse emission from SgrA East and West and from the molecular clouds in this region (SgrB2, SgrC, SgrD) will be reported in a separate paper.

2. Observations

The *BeppoSAX* satellite (Boella et al. 1997a) carries a complement of several imaging and non-imaging X-ray detectors, covering a broad energy range from 0.1 keV to 300 keV. Most of the results presented here have been obtained with the imaging instruments placed in the focal planes of four identical X-ray Mirror Units: the Medium-Energy Concentrator Spectrometer (MECS, Boella et al. 1997b) and the Low-Energy Concentrator Spectrometer (LECS, Parmar et al. 1997). Each Mirror Unit consists of 30 nested, confocal mirrors with a double cone approximation to the Wolter I geometry and a focal length of 185 cm.

The MECS instrument is based on three position-sensitive gas-scintillation proportional counters, providing 1.3–10 keV images over a field of view with $\sim 28'$ radius. The MECS is characterized by a total (three telescopes) effective area of $\sim 150 \text{ cm}^2$ at 6 keV, a relatively good angular resolution (50% power radius of $\sim 75''$ at 6 keV, on-axis) and a moderate energy resolution (FWHM $\sim 8.5\sqrt{6/E_{\text{keV}}}\%$). One (M1) of the three nearly identical units composing the MECS had a failure in May 1997; all the observations performed after that date were carried out only with the remaining two units (M2 and M3).

The fourth Mirror Unit is associated with the LECS instrument. This consists of a position-sensitive gas-scintillation proportional counter utilizing an ultra thin, organic detector entrance window (1.25 μm) and a driftless configuration to extend the low energy

response down to 0.1 keV. Its spatial and energy resolutions are similar to those of the MECS, but the field of view is slightly smaller ($\sim 18'$ radius). Due to UV contamination leaking through the entrance window during sunlit periods, the LECS is operated only at satellite night time, resulting in effective exposure times smaller than those of the other *BeppoSAX* instruments (typically $\sim 50\%$ of the MECS values).

For the analysis of 1E 1740.7–2942, which has a hard spectrum extending above the MECS energy range we have also used the Phoswich Detector System instrument (PDS, Frontera et al. 1997). This non-imaging instrument points in the same direction of the MECS and LECS telescopes and covers the 15–300 keV energy range. It consists of a square array of four independent NaI(Tl)/CsI(Na) phoswich scintillation detectors equipped with collimators defining a field of view of $\sim 1.3^\circ$ (FWHM). There are two separate collimators, one for each pair of detectors, that can be independently rocked off-axis to monitor the background. During our observations the default rocking mode with offset angles of $\pm 210'$ and dwell time 96 s was used. The PDS provides an energy resolution of $\sim 15\%$ at 60 keV (FWHM).

The log of our *BeppoSAX* observations of the GC region performed in 1996–98 is shown in Table 1. The pointing directions were chosen to cover a $\sim 4^\circ$ long region at $b=0^\circ$, as well as a few known sources slightly outside the galactic plane. We chose to partially overlap adjacent pointings, in order to continuously cover the galactic plane with the central part of the MECS field of view ($\sim 8'$ radius), where the instrument sensitivity and angular resolution are best. As shown in Table 1, a few pointing directions were observed twice, at time intervals of 6 or 12 months. This was partly planned, to study the long term variability of the sources, and partly resulted from operational constraints. The exposure time achieved in the different regions is not uniform, ranging from a minimum of 7 ks to ~ 340 ks at the position of 1E 1743.1–2843.

An exposure-corrected mosaic of the MECS images in the 2–10 keV energy range is shown in Fig. 1.

EDITOR: PLACE TABLE 1 HERE.

3. Data Analysis

Except where noted, the spectral analysis of all the point sources reported here has been carried out as follows: the LECS and MECS counts have been extracted from a circular region with $4'$ radius centered at the position of the source and rebinned in order to have at least 20 counts per energy bin. The $4'$ radius corresponds to an encircled energy of 90%. In several cases we used a smaller extraction radius ($2'$, $\sim 60\%$ enclosed energy) in order to reduce the problems due to source crowding or unfavourable locations in the MECS field of view.

In any case the response matrices appropriate to the adopted extraction radius and source position on the detector have been used. While these matrices include the elements to properly derive the correct spectral shape of the sources observed off-axis, the resulting fluxes can be affected by an uncertainty in their absolute normalization that in some cases could reach $\sim 40\%$.

From each spectrum we have subtracted a local background, extracted from a source free region of the same observation: in fact, the standard *BeppoSAX* background spectra obtained from blank field observations underestimate the actual background present in the GC region, which is dominated by the galactic diffuse emission.

The PDS data were reduced using the SAXDAS software package (Version 1.2.0). The time intervals before and after Earth occultations were excluded and the spurious spikes

(Guainazzi & Matteuzzi 1997) filtered out. The background subtraction was performed with the standard rocking collimator technique. The background-subtracted spectra were rebinned in order to have at least 100 counts for each energy channel and then analyzed using the response matrix released on August 31, 1997.

The resulting LECS/MECS/PDS spectra have been fitted with different models implemented in XSPEC (Version 10.00). We took into account the known intercalibration normalizations between the different instruments on-board *BeppoSAX* (Fiore, Guainazzi & Grandi 1999), using different relative normalizations $A_{LECS} \sim 0.85$, $A_{MECS}=1$ and $A_{PDS} \sim 0.8$. MECS spectra were extracted in the 2–10 keV energy range, while for the LECS we used only the data below 2 keV (we verified that using the LECS data above this energy did not significantly improve the results obtained with the MECS).

4. Results

Several previously known sources have been observed in our *BeppoSAX* pointings: 1E 1743.1–2843 (Watson et al. 1981), the persistent black hole candidate 1E 1740.7–2942 (Sunyaev et al. 1991a), the X-ray bursters SLX 1744–299, SLX 1744–300, A 1742–294, KS 1741–293 (Skinner et al. 1990; Pavlinsky, Grebenev & Sunyaev 1994; Kawai et al. 1988), and the source(s) at the GC position (Watson et al. 1981). We also detected two X-ray transients discovered very recently: SAX J1747.0–2853 (in't Zand et al. 1998b) and XTE J1748–288 (Smith, Levine & Wood 1998), and discovered a new X-ray source that we identified as the plerionic emission from the composite supernova remnant G0.9+0.1 (Mereghetti, Sidoli & Israel 1998).

All the sources observed in our survey are listed in Table 2. Note that in Table 2 we have reported the best source positions and corresponding uncertainties available in the

literature. The positions derived from our analysis have typical uncertainties of the order of $\sim 1'$ (95% confidence level) and are in agreement with those of Table 2. We have listed in Table 2 also the positions of a few other objects which are relevant in the following discussion of the sources near SgrA*.

The results for the individual sources are reported in the following sections, while in Table 3 we have summarized the parameters of the best fits. All the luminosities are given for an assumed distance of 8.5 kpc, unless stated differently.

EDITOR: PLACE TABLE 2 HERE.

EDITOR: PLACE TABLE 3 HERE.

4.1. The source(s) at the Galactic Center position (1E 1742.5–2859)

The GC field was observed for 100 ks in August 1997 (Obs. n.3). Strong X-ray emission peaked at the GC position is clearly detected with the LECS and MECS instruments. The central part of the MECS image is shown in Fig. 2, where the positions of the X-ray sources previously detected with other satellites have been indicated. The background subtracted radial profiles of the X-ray emission in the soft (2–5 keV) and hard (5–10 keV) energy ranges are shown in Fig. 3. The data points represent the surface brightness measured in concentric rings centered at the position of SgrA*, while the solid lines show for comparison the profiles expected from a single unresolved point source. The expected profiles have been normalized to yield the same number of counts within $10'$ as the measured data. It is clear that the shape of the observed profiles is incompatible with a single point-like source. The observed radial profile results from the contribution of a diffuse component and one (or possibly more) sources close to the SgrA* position.

EDITOR: PLACE FIGURE 2 HERE.

EDITOR: PLACE FIGURE 3 HERE.

The X-ray images of this region with the best angular resolution available so far are those obtained with the ROSAT PSPC instrument (Predehl & Trumper, 1994) which, in addition to the diffuse emission, showed the presence of three different sources. Their error regions ($20''$ radius) are indicated in Fig. 2 with the small circles labelled PT6, PT7 and PT8. One of these sources (PT7) is highly absorbed and located within $10''$ from Sgr A*, while PT6 has been interpreted as a foreground star, due to its smaller column density. It is evident that the emission detected with *BeppoSAX* is peaked at the position of PT7, although we cannot exclude that also the other ROSAT sources (and AX J1745.6–2901, see below) contribute to some of the detected X-rays.

Though the limited angular resolution hampers a detailed analysis and introduces unavoidable uncertainties, we proceeded as follows to estimate the spectrum and flux to be ascribed to the GC point source(s).

A spectrum was extracted from a circular region with $2'$ radius centered at the position of the X-ray peak flux (see Fig. 2). The background was taken from an external annular region ($6' - 8'$), in order to subtract the contribution from the diffuse emission.

A power law does not give an appropriate fit to the resulting spectrum, which clearly shows evidence for emission lines at 6.7 keV and also at lower energies, indicative of a possible thermal origin of the emission. The sulfur line at ~ 2.4 keV is particularly bright. A power law with a gaussian line at 6.7 keV gives a better result, with a photon index $\Gamma \sim 2.6$ and a column density $N_H \sim 8 \times 10^{22} \text{ cm}^{-2}$ ($\chi^2 = 1.1$). When the centroid energy and width of the gaussian are let free in the fit, we obtain the values $E=6.7$ keV, $\sigma=13$ eV

and an equivalent width $EW \sim 1.2$ keV. The same results were found fixing the σ of the iron line at 0. No evidence for a 6.4 keV line of fluorescent origin is present, contrary to what is found in the surrounding diffuse emission (a detailed study of which is deferred to a separate paper). The 2–10 keV flux corrected for the absorption is $\sim 4 \times 10^{-11}$ ergs $cm^{-2}s^{-1}$ and the luminosity is $\sim 3 \times 10^{35}$ ergs s^{-1} at a distance of 8.5 kpc.

EDITOR: PLACE FIGURE 4 HERE.

We also fitted the data with a thermal plasma model (MEKAL in XSPEC, Mewe, Gronenschild & van den Oord 1985). It properly accounts for the 6.7 keV iron emission line, but leaves some residuals around 2.4 keV (see Fig. 4), possibly indicating the presence of a multitemperature plasma. In order to properly account for the emission lines at lower energies, we fitted the spectrum with the sum of two MEKAL components with different temperatures ($kT_{M1} \sim 0.8$ keV and $kT_{M2} \sim 5$ keV), obtaining a higher N_H . Also a single MEKAL model ($kT_M \sim 1.3$ keV) plus a power law with a gaussian added at 6.7 keV fit well the data. All the spectral results are summarized in Table 3.

4.2. AX J1745.6–2901

During observations of the GC region performed with the ASCA satellite in 1993 and 1994 a possibly new source was discovered $\sim 1.3'$ SW of SgrA* (Maeda et al. 1996). The spectrum of this source, later named AX J1745.6–2901 (Maeda et al. 1998), was harder than that of the X-ray emission coming from the position of Sgr A*. AX J1745.6–2901 varied by a factor ~ 5 in flux between the two observations separated by one year, and it showed an X-ray burst and periodic (8.4 hr) eclipses (Maeda et al. 1996). These authors proposed that AX J1745.6–2901 could be the quiescent counterpart of the bright soft X-ray transient A1742-289 observed in outburst in 1975 (Eyles et al. 1975, Branduardi et al.

1976). However, the absence of eclipses at the 8.4 hr period in the Ariel V archival data of the A1742-289 outburst (Kennea & Skinner 1996), makes this association uncertain. It is therefore likely that AX J1745.6–2901 is a different neutron star LMXRB.

In order to search for the possible presence of AX J1745.6–2901 in our observations, we compared the MECS images accumulated in the soft (2–6 keV) and hard (6–10 keV) energy ranges. This was done independently for the two MECS units (M2 and M3) to obtain the best angular resolution by avoiding possible small misalignment errors. Furthermore, we selected only time intervals in which the *BeppeSAX* attitude was determined with two star trackers (indeed small deviations $\lesssim 2'$ may be present when no star tracker is active or when only one is in use).

EDITOR: PLACE FIGURE 5 HERE.

The resulting images for the M3 unit are shown in Fig. 5. In the high energy image, an excess emission in the SW direction is clearly resolved from the softer (and partly diffuse) emission due to the 1E 1742.5–2859 (GC) source(s). The position of this excess is consistent with that of AX J1745.6–2901. It is visible only in the higher energy channels of M3: in fact the higher background due to misplaced events from the iron calibration sources prevents its detection also in M2 (Chiappetti et al. 1998).

The weakness of the source and the presence of the nearby much brighter X-ray emission hampers an accurate determination of its flux and spectrum, which, in any case, is consistent with the lower value observed with ASCA in 1993 (Maeda et al. 1996).

4.3. 1E 1740.7–2942

We obtained two observations (Obs. n. 1 and 6) pointed on the “microquasar” source 1E 1740.7–2942 (Mirabel et al. 1992). Our spectral analysis is based on the longer observation performed in September 1997.

As shown by previous observations with coded mask imaging instruments in the hard X-ray band (Skinner et al. 1987, Goldwurm et al. 1994), 1E 1740.7–2942 is the strongest persistent source at energies greater than ~ 30 keV within a few degrees from the GC. We therefore analyzed also the PDS data, in which the source was clearly detected up to ~ 150 keV. Due to the crowding of this region of the sky, particular care was devoted to the analysis of this non-imaging detector. The PDS field of view includes the positions of the persistent LMXRB A 1742–294 and of the transient KS 1741–293. As shown by our simultaneous MECS data, the latter source was not active at the time of observation. A 1742–294 lies at $\sim 30'$ from 1E 1740.7–2942 and it has a similar flux in the 2–10 keV range. However, it has a much softer spectrum (see Table 3). Using our best fit thermal bremsstrahlung results and taking into account the reduced off-axis response of the PDS collimator, we estimate that A 1742–294 contributes less than 10% to the observed counts above 40 keV. A further problem arised by the contamination of one of the two offset collimator positions used in the background determination by the bright X-ray source GX 3+1. We therefore estimated the PDS background using only one of the two off-axis collimator positions.

A single power law provides an adequate fit to the LECS and MECS spectrum below 10 keV (photon index $\Gamma \sim 1.5$, $N_H \sim 1.5 \times 10^{23}$ cm $^{-2}$). We searched in the MECS data for the possible presence of iron lines obtaining a negative result: for lines in the range 6.4–6.7 keV we can give a 90% upper limit to the equivalent width of ~ 30 eV (with a line width σ fixed at 0). This upper limit increases up to ~ 50 eV for $\sigma = 500$ eV. These results are

similar to the findings of Sakano et al. (1999) who recently reanalyzed all the ASCA data on 1E 1740.7–2942.

However, a single power law cannot provide an adequate fit over the broad energy range covered by BeppoSAX. In fact the inclusion of the PDS data clearly shows the presence of a spectral turn over at higher energies (see Fig. 6). Good fits could be obtained with a power law with an exponential cut-off or with Comptonization models (see Table 3).

1E 1740.7-2942 is of particular interest since, beside being one of the few galactic objects with persistent hard X-ray emission extending above \sim 100 keV, it has a peculiar radio counterpart with double sided relativistic jets (Mirabel et al. 1992). The observation of a transient broad spectral feature at \sim 480 keV (Bouchet et al. 1991), suggested that 1E 1740.7-2942 might be related to the 511 keV line observed from the GC region. On the basis of these properties and of its hard X-ray spectrum similar to that of Cyg X-1, 1E 1740.7-2942 is generally considered a black hole candidate. The broad band spectrum measured with BeppoSAX is consistent with this interpretation.

EDITOR: PLACE FIGURE 6 HERE.

4.4. A 1742–294

A 1742–294, although sometimes referred to as a transient source, has always been detected in all the GC observations since 1975 (see references in van Paradijs 1995).

It was observed twice in the outer part of the MECS field of view (Obs. n. 8 and 9). In the 1997 observation A 1742–294 was very close to the region of the field of view used for the on board calibration sources. So we extracted the counts for the spectral analysis from a small circular region with 2' radius. In both observations acceptable fits were obtained

both with a power law and with a thermal bremsstrahlung (see Table 3). In March 1998 the source was softer and brighter (of roughly a factor of two). Moreover, some variability on a time scale of hours was observed during both observations (see the light curves in Fig. 7).

We detected three type I X-ray bursts from A 1742–294: one on September 16 (20:04:04 UT) and two on March 31, 1998 (9:44:58 UT and 15:01:20 UT). The poor statistics hampers a detailed study of the neutron star luminosity, radius and temperature variations during the bursts.

EDITOR: PLACE FIGURE 7 HERE.

4.5. SLX 1744–299 and SLX 1744–300

SLX 1744–299, first discovered with the Spartan 1 experiment (Kawai et al. 1988), was subsequently resolved into two distinct objects separated by $\sim 2.5'$ with the SL2-XRT coded mask telescope (Skinner et al. 1987, 1990).

We obtained a single observation pointed on these two sources in September 1997 (Obs. n.7). For the spectral analysis we used extraction radii of only $2'$, and the same background estimated from a circular corona surrounding both sources. Though the results have to be taken with some caution due to the unavoidable cross-contamination of the two spectra, we can safely conclude that SLX 1744–300 is fainter and has a slightly softer spectrum than SLX 1744–299. However, contrary to Predehl et al. (1995), we cannot claim a significant difference in their absorption column densities (see results in Table 3).

Though both SLX 1744–299 and SLX 1744–300 have been reported to emit X-ray bursts (Skinner et al. 1987, 1990; Sunyaev et al. 1991b), none was detected during our observation.

4.6. XTE J1748–288

This transient source was discovered with the RossiXTE satellite in June 1998 (Smith, Levine & Wood 1998). Its hard X-ray spectrum and its association with a variable radio source with evidence for the presence of jets establish XTE J1748–288 as a possible black hole candidate (Strohmayer & Marshall 1998, Hjellming et al. 1998, Fender & Stappers 1998).

We detected XTE J1748–288 in the August 1998 observation (Obs. n.11). Its spectrum, extracted from a $2'$ radius region to avoid the problems due to the poorly known additional absorption from the strongback support of the MECS detector entrance window, could be fit equally well by a hard power law (photon index ~ 1.5) or by a thermal bremsstrahlung with $kT \sim 40$ keV. The flux was $\sim 10^{-10}$ erg cm $^{-2}$ s $^{-1}$ (2–10 keV, corrected for the absorption). The light curve of the XTE J1748–288 outburst obtained with the RossiXTE ASM is shown in Fig. 8. The date of our observation and the measured flux are indicated by the dashed lines, showing that we obtained a positive detection of XTE J1748–288 when it was well below the ASM sensitivity threshold. It is interesting to note that the flux measured with *BeppoSAX* is consistent with the extrapolation of the decaying light curve observed with the ASM until about mid-July. This suggests that the nearly exponential decay, with e-folding time ~ 20 days, lasted until the date of our observation (August 26th).

EDITOR: PLACE FIGURE 8 HERE.

4.7. SAX J1747.0–2853

The source SAX J1747.0–2853, positionally consistent with the transient GX 0.2–0.2 observed in 1976 (Proctor, Skinner & Willmore 1978), was discovered with the *BeppoSAX*

Wide Field Camera (WFC) instrument during an outburst in March 1998 (in't Zand et al. 1998b, Bazzano et al. 1998).

EDITOR: PLACE FIGURE 9 HERE.

During our observation pointed on 1E 1743.1–2843 (Obs. n.10), SAX J1747.0–2853 was detected at an off-axis angle of $\sim 13'$. During this observation, performed about 20 days after the WFC ones, a Type-I X-ray burst from this source was seen (Sidoli et al. 1998b). The burst, starting at 1:40 UT of 1998 April 15, was also visible at energies above 10 keV with the PDS instrument. The burst light curve in different energy ranges is shown in Fig. 9, where we also present the variations of the spectral fit parameters during the burst (see Sidoli et al. 1998b for details). The spectral softening clearly indicates that the burst is of Type I, confirming the LMXRB nature of this source. Assuming an Eddington luminosity at the burst peak, we obtain a distance of ~ 10 kpc, and a blackbody radius consistent with the expectations for a neutron star.

4.8. KS 1741–293

During our observation pointed on the molecular cloud SgrC performed in March 1998 (Obs. n.9), we detected a source positionally coincident with the transient burster KS1741-293 (in't Zand et al. 1998c).

Since the source was located close to the strongback support of the MECS detector entrance window, we used a small extraction radius ($2'$) for the spectral analysis. The background was estimated locally from a source free region of the same observation. The spectrum is relatively soft and could be described equally well by a power law and a thermal bremsstrahlung (see Table 3), giving in both cases a high column density $N_H \sim 2 \times 10^{23}$

cm^{−2}, and a luminosity $L_X \sim 10^{36}$ erg s^{−1} (2–10 keV, corrected for absorption). Slightly lower column densities and luminosity were obtained with a blackbody spectrum (see Table 3).

The same region of sky was observed by *BeppoSAX* in September 1997 (Obs. n.8) and KS 1741–293 was not detected, with an upper limit of $L_X < 10^{35}$ erg s^{−1}.

4.9. 1E 1743.1–2843

This bright and highly absorbed source has been repeatedly observed in several of our pointings. The best fit results reported in Table 3 refer to the observation performed in April 1998 (Obs. n.11), in which 1E 1743.1–2843 was on-axis. This source is probably a persistent LMXRB, though no X-ray bursts have been detected so far. For a complete discussion of all the *BeppoSAX* and ASCA observations of 1E 1743.1–2843 see Cremonesi et al. (1999).

4.10. The supernova remnant G0.9+0.1

The discovery of X-ray emission from the center of the radio supernova remnant G0.9+0.1 has been reported by Mereghetti, Sidoli & Israel (1998). The location of G0.9+0.1 was imaged in April and September 1997, during observations pointed on the Sgr B2 molecular cloud. The angular resolution of the MECS at the off-axis location of G0.9+0.1 ($\sim 14'$) only allowed to establish that the X-ray emission is associated with the plerionic radio core of the supernova remnant and not with the surrounding shell ($\sim 8'$ diameter, Helfand & Becker 1987). However, it was not possible to discriminate between a point source (i.e. a neutron star) and a synchrotron nebula of a few arcmin extent.

We have performed a new spectral analysis based on the improved calibration results that are now available. The derived spectral parameters are within the uncertainties of those previously reported (Mereghetti, Sidoli & Israel 1998), but they are more precise.

The best fit power-law spectrum has a photon index $\Gamma = 2.5$, $N_H = 2.5 \times 10^{23} \text{ cm}^{-2}$, and flux $F = 2 \times 10^{-11} \text{ erg cm}^{-2} \text{ s}^{-1}$ (2–10 keV, corrected for the absorption). Equally good fits were also obtained with blackbody and thermal bremsstrahlung spectra (see Table 3), while a Raymond-Smith thermal plasma model with abundances fixed at the solar values gave a worse result.

The *BeppoSAX* discovery of X-ray emission from the central region of G0.9+0.1 confirms its plerionic morphology derived from the radio observations. The presence of a young, energetic pulsar in G0.9+0.1 could also explain part of the high energy gamma-ray emission observed with EGRET from the region of the Galactic Center (Mayer-Hasselwander et al. 1998).

4.11. G359.23–0.92 (The Mouse)

The radio source G359.23–0.92, also known as the Mouse, belongs to a small class of radio nebulae characterized by an axially symmetric morphology (Yusef-Zadeh & Bally 1987). It is believed that these sources are produced by relativistic particles ejected by a compact object (either a pulsar or a binary system) moving with high speed along the axis of symmetry (Shaver et al. 1985, Helfand & Becker 1985). Predehl & Kulkarni (1995) using the ROSAT PSPC instrument discovered X-ray emission associated with the “head” of the Mouse, located only $2.3'$ northeast of SLX 1744–299. Since the MECS data of SLX 1744–299/300 showed some evidence for an elongation in the direction of G359.23–0.92, we performed the same procedure described in section 4.2 for AX J1745.6–2901. The

resulting 6–10 keV image, shown in Fig. 10, confirms the MECS detection of G359.23–0.92.

EDITOR: PLACE FIGURE 10 HERE.

To estimate the spectral parameters of G359.23–0.92 we used a small extraction radius ($2'$) and measured the background (which is dominated by the counts of the nearby sources) from a similar region at the same distance from SLX 1744–299. A power law fit gave $\Gamma \sim 1.9\text{--}2.3$, a column density of $4\text{--}6 \times 10^{22} \text{ cm}^{-2}$ and an unabsorbed flux in the 2–10 keV band of the order of $3 \times 10^{-11} \text{ erg cm}^{-2} \text{ s}^{-1}$.

This flux is higher than the value expected based on the ROSAT results at energies below 2.4 keV (Predehl & Kulkarni 1995), however this discrepancy might be due to different reasons other than source variability. First, the flux reported by these authors was based on the assumption of a value of only $2 \times 10^{22} \text{ cm}^{-2}$ for the column density: we found that for our N_H value the MECS and ROSAT PSPC count rate are consistent with the same flux level. Another possibility is that we underestimated the contamination from SLX 1744–299/300.

In any case, the detection at energies greater than 6 keV is statistically significant and supports a non-thermal origin for the X-ray emission from the head of the “Mouse”.

5. Discussion

Our *BeppoSAX* survey of the inner 4 degrees of the galactic plane shows that a few persistently bright sources characterize the constellation of X-ray sources near the GC. Their properties indicate that they consist of compact accreting objects similar to the classical accretion powered sources found elsewhere in the Galaxy. Both systems containing neutron stars (e.g. SLX 1744–299/300, A 1742–294) and likely black holes (1E 1740.7–2942

) are present.

However, these persistently bright objects represent only a small fraction of the X-ray sources in this region. Three transient sources (SAX J1747.0–2853, KS 1741–293 and XTE J1748-288) were detected in our survey, but it is known from previous observations that many more are present. We therefore confirm the clustering of X-ray sources towards the GC already noted by several authors.

It is likely that on the large scale (\sim degrees) this simply reflect the general mass distribution enhancement, as found by Grebenev, Pavlinsky & Sunyaev (1996) who considered only the hard X-ray sources detected with the ART-P coded mask telescope. On the other hand, considering the distribution of all the sources reported within several arcminutes from SgrA* there is marginal evidence of an additional source population (Skinner 1993). However, this conclusion might be biased by the different sensitivity and angular resolution of the many observations of this field. Though it is obvious that the regions closer to the center have been observed more deeply, the effect of this bias is difficult to quantify. We finally note that the case of the three sources in the direction of SLX J1744–299/300 (at $b = -1.5^\circ$) is maybe more surprising that the presence of 4-5 sources close to SgrA*. While G359.23–0.92 is very likely a foreground object, the two X-ray bursters SLX J1744–299 and SLX J1744–300 could be at the same distance and therefore somehow related (e.g. members of a star cluster). Observations in X-rays with better angular resolution and deep searches in the infrared are needed to study these objects.

EDITOR: PLACE FIGURE 11 HERE.

In Fig. 11 we have plotted the column density and power law photon index (in the 2–10 keV range) for all the sources that we have observed (to compare the spectra of the different sources, we have used a power law also in a few cases in which other models

provided better fits). It is clear that sources containing neutron stars, as indicated by the presence of Type I bursts, have softer spectra than the black hole candidates. Based on this spectral dichotomy, it is likely that also 1E 1743.1-2843 contain a neutron star. Fig. 11 also shows that the column densities of these sources vary over a factor ~ 4 range. This is probably related to the clumpiness of the molecular clouds in this region rather than to a corresponding spread in the source distances.

5.1. Sgr A* and the galactic center X-ray source(s)

At least four point sources (Predehl & Trumper 1994, Maeda et al. 1996), maybe five (Kennea & Skinner 1996) and possibly more could contribute to the X-ray flux detected with *BeppoSAX* when pointing at the GC, in addition to the diffuse emission that permeates the region (Maeda & Koyama 1996). However, as shown in Fig 2, the MECS source position is closer to the ROSAT counterpart of SgrA* than to the other two ROSAT sources (PT6 and PT8).

The emission lines detected in the MECS spectrum within $2'$ from the GC clearly indicate a substantial contribution from the thermal diffuse emission associated to the SgrA West and SgrA East regions (Yusef-Zadeh et al. 1997). Unfortunately, this contribution is difficult to quantify, and the limited angular resolution does not allow to measure the flux to be ascribed to SgrA* itself.

We can place a very conservative upper limit to the luminosity of SgrA* by assuming that it is the only point source and that the diffuse emission at its position has the same surface brightness of the annular region ($6' - 8'$) described above. In this case, using the flux reported in Table 3, we obtain a luminosity of $\sim 3 \times 10^{35}$ ergs s^{-1} (2–10 keV, corrected for the absorption). However, this is probably an overestimate of the true luminosity of SgrA*

for the fact that the diffuse emission has a surface brightness distribution that increases toward the GC and because there might be a contribution from the other point sources.

A more realistic upper limit to the X-ray emission from SgrA* can be placed if we consider an X-ray background rising towards the GC: we measured the surface brightness from three concentric annular regions ($2' - 4'$, $4' - 6'$ and $6' - 8'$) and extrapolated it at our source position. In this case we find a new background value, four times higher than the previous one and the new flux for the point source is $\sim 1.5 \times 10^{-11}$ ergs cm $^{-2}$ s $^{-1}$, that translates into a luminosity at 8.5 kpc of $\sim 10^{35}$ ergs s $^{-1}$. This upper limit is similar to the value reported by the ASCA team (Maeda et al., 1998) and is well below the Eddington luminosity for a super-massive black hole.

Several authors tried to explain this high energy underluminosity of SgrA* with different models for the accretion, from a spherical accretion (Melia 1992) to the advection dominated accretion flow (Narayan, Yi & Mahadevan 1995; Narayan et al. 1998). These models have still some problems in the radio and in the γ -ray bands (EGRET source 2EG 1746–2852), where substantial excesses are present. Several solution has been proposed: the inclusion of an emission process associated with protons (Mahadevan et al. 1998) is able to solve the problem of the radio excess, while the EGRET source is considered as a gamma-ray upper limit due to the poor spatial resolution. Another possible explanation is that the EGRET source is not related with SgrA*, but with the SgrA East supernova remnant shell (Melia et al. 1998).

The XMM and AXAF observatories with their superior imaging capabilities will substantially contribute to solve the problem of the high energy emission from SgrA* and put more stringent constraints to the accretion models.

We thank Silvano Molendi for useful discussions and help with the data analysis.

Table 1. BeppoSAX observations summary.

Obs. n.	Pointing Direction R.A. and Dec. (J2000)	Observation Date Start & Stop time (UT)	MECS Exposure Time (ks)	Main target
1	17 43 54.8 –29 44 42	1996 Sep 03 10:56 - 03 16:30	7	1E 1740.7–2942
2	17 47 20.0 –28 24 02	1997 Apr 05 08:57 - 06 09:33	49	Sgr B2
3	17 45 40.3 –29 00 23	1997 Aug 24 06:01 - 26 08:41	100	Sgr A*
4	17 47 20.0 –28 24 02	1997 Sep 03 05:18 - 04 09:36	51	Sgr B2
5	17 48 39.2 –28 05 56	1997 Sep 04 22:45 - 06 03:22	49	Sgr D
6	17 43 54.8 –29 44 42	1997 Sep 07 05:45 - 08 06:57	43	1E 1740.7–2942
7	17 47 25.8 –30 01 01	1997 Sep 10 14:07 - 11 18:36	21	SLX 1744–299
8	17 44 41.3 –29 28 14	1997 Sep 16 11:30 - 16 20:47	15	Sgr C
9	17 44 41.3 –29 28 14	1998 Mar 31 06:47 - 31 20:54	25	Sgr C
10	17 46 19.9 –28 44 00	1998 Apr 13 13:36 - 15 05:51	71	1E 1743.1–2843
11	17 46 50.2 –28 33 04	1998 Aug 26 16:34 - 28 16:30	79	Sgr B1

Table 2. X-ray sources in the observed region.

Source	RA (J2000)	Dec (J2000)	Error	Notes	Ref. ^a
XTE J1748–288	17 48 08	-28 28 48	1'	Transient	1
SLX 1744–299	17 47 27	-29 59 55	1'	Burster	2
SLX 1744–300	17 47 27	-30 02 15	1'	Burster	2
G0.9+0.1	17 47 21	-28 09 22		SNR	3
G359.2–0.8 (The Mouse)	17 47 15.2	-29 58 00	8''		4
SAX J1747.0–2853	17 47 0	-28 52 12	1'	Transient/Burster	5
1E 1743.1–2843	17 46 19.5	-28 53 43	1'		6
A 1742–294	17 46 05	-29 30 54	1'	Burster	7
RXJ 1745.7–2858	17 45 45.5	-28 58 17	20''	Star? (PT6)	8
1E 1742.5–2859	17 45 40.7	-29 00 10	1'	SgrA*?	6
RXJ 1745.6–2900	17 45 40.4	-29 00 23	20''	SgrA*? (PT7)	8
AX J1745.6–2901	17 45 36	-29 01 34	25''	Transient/Burster?	9
RXJ 1745.5–2859	17 45 32	-28 59 29	20''	PT8	8
A 1742–289	17 45 37.3	-29 01 04.8	2.8''	Transient	10
KS 1741–293	17 44 49.2	-29 21 06.3	1'	Transient/Burster	11
1E 1740.7–2942	17 43 54.8	-29 44 42.8	1''	Black hole candidate	12

^aReferences are: 1=Strohmayer & Marshall 1998, 2=Skinner et al. 1990, 3=Helfand & Becker 1987, 4=Predehl & Kulkarni 1995, 5=Bazzano et al. 1998, 6=Watson et al. 1981, 7=Pavlinsky, Grebenev & Sunyaev 1994, 8=Predehl & Trumper 1994, 9=Maeda et al. 1996, 10=Davies et al. 1976, 11=In't Zand et al. 1990, 12=Mirabel et al. 1992

Table 3. Results of the Spectral Fits (errors are 90% confidence level).

Source (data)	Model ^a	Column density (10^{22} cm $^{-2}$)	Parameter ^b	Red. χ^2 (d.o.f.)	Flux ^c
Galactic center (MECS)	PL+line(6.7)	8.3 ± 0.5	$\Gamma = 2.6 \pm 0.1$ $EW(6.7) = 1.2$	1.12 (284)	4.0 ± 0.2
	Brems+line(6.7)	6.6 ± 0.3	$T = 5.1 \pm 0.5$ $EW(6.7) = 1.2$	1.20 (284)	3.3 ± 0.2
	M	7.0 ± 0.3	$T = 4.1 \pm 0.3$	1.16 (288)	3.5 ± 0.2
	M+M	11.3 ± 1.2	$T_{M1} = 0.80^{+0.18}_{-0.08}$ $T_{M2} = 4.9 \pm 0.4$	1.00 (285)	$6.0^{+0.6}_{-1.0}$
	M+PL+line(6.7)	10 ± 1	$T_M = 1.3^{+0.2}_{-0.6}$ $\Gamma = 1.7 \pm 1$ $EW(6.7) = 0.7 - 1$	0.97 (281)	5.5 ± 1
1E 1740.7-2942 (MECS)	PL	14.7 ± 0.4	$\Gamma = 1.52 \pm 0.04$	1.10 (180)	49.5 ± 1.0
	Brems	14.1 ± 0.3	$T = 34.5 \pm 6.0$	1.12 (180)	47.4 ± 0.4
(LECS+MECS +PDS)	PL	14.5 ± 0.3	$\Gamma = 1.45 \pm 0.3$	2.84 (283)	49 ± 1
	Brems	12.9 ± 0.2	$T = 174 \pm 6$	1.80 (283)	45 ± 0.5
	CompST	14.6 ± 0.2	$T = 24 \pm 1$ $\tau = 5.5 \pm 0.1$	1.30 (282)	49 ± 0.5
	PL+E _c	13.6 ± 0.2	$\Gamma = 1.36 \pm 0.02$ $E_c = 52 \pm 4$ $E_{fold} = 105 \pm 10$	1.24 (281)	46.7 ± 0.5
A 1742-294 (MECS-Obs.9)	PL	6.5 ± 0.5	$\Gamma = 1.72 \pm 0.11$	0.995 (238)	30 ± 1
	Brems	5.9 ± 0.4	$T = 16.3^{+5.1}_{-3.6}$	0.986 (238)	29 ± 1
	PL	6.9 ± 0.3	$\Gamma = 1.97 \pm 0.05$	0.99 (323)	63 ± 1
(MECS-Obs.10)	Brems	6.0 ± 0.2	$T = 10.3 \pm 1.0$	1.01 (323)	58 ± 1
SLX 1744-299 (MECS)	PL	5.1 ± 0.2	$\Gamma = 2.1 \pm 0.1$	0.92 (364)	20 ± 0.4
	Brems	4.2 ± 0.2	$T = 8.9 \pm 0.6$	0.99 (364)	18 ± 0.4
SLX 1744-300 (MECS)	PL	5.3 ± 0.2	$\Gamma = 2.2 \pm 0.1$	1.06 (342)	12 ± 0.3
	Brems	4.2 ± 0.2	$T = 7.7 \pm 0.5$	1.09 (342)	11 ± 0.3

Table 3—Continued

Source (data)	Model ^a	Column density (10^{22} cm $^{-2}$)	Parameter ^b	Red. χ^2 (d.o.f.)	Flux ^c
XTE J1748–288 (MECS)	PL	7.3 ± 0.5	$\Gamma = 1.46 \pm 0.1$	0.922 (163)	11.2 ± 0.3
	Brems	6.9 ± 0.4	$T = 40^{+24}_{-11}$	0.93 (163)	10.9 ± 0.3
SAX J1747.0–2853 (MECS)	Brems	$8.3^{+0.6}_{-0.3}$	$T = 6.1^{+0.9}_{-0.7}$	1.01 (138)	$4.0^{+0.2}_{-0.3}$
	PL	20 ± 2	$\Gamma = 2 \pm 0.2$	0.992 (213)	$14.5^{+2.0}_{-0.6}$
(MECS)	Brems	18 ± 1	$T = 11 \pm 3$	0.917 (213)	$12.5^{+1.2}_{-0.5}$
	BB	12 ± 2	$T = 1.8 \pm 3$	0.966 (213)	8.5 ± 0.4
1E 1743.1–2843 (MECS)	BB	13 ± 1	$T = 1.8 \pm 1$	1.01 (178)	16.5 ± 0.5
	PL	25^{+17}_{-10}	$\Gamma = 2.5^{+1.5}_{-0.8}$	0.72 (28)	$2.0^{+4.0}_{-1.0}$
(MECS)	Brems	23^{+12}_{-8}	$T = 6^{+13}_{-3}$	0.72 (28)	$1.5^{+0.2}_{-0.5}$
	BB	16^{+10}_{-10}	$T = 1.6^{+0.6}_{-0.5}$	0.72 (28)	$0.9^{+0.2}_{-0.4}$
G359.23-0.92 (MECS)	PL	$4 - 6$	$\Gamma = 1.9 - 2.3$		~ 3

^aPL=Power Law, PL+E_c= Power law plus high energy cutoff (E_c=cutoff energy in keV; E_{fold}=e-folding energy in keV), BB=Blackbody, Brems=Thermal Bremsstrahlung, CompST=Comptonization model (Sunyaev & Titarchuk 1980), line=gaussian line, M=MEKAL model in XSPEC.

^bAll the temperatures and energies are in keV, Γ =photon index.

^cUnabsorbed fluxes (2–10 keV) are in units of 10^{-11} ergs cm $^{-2}$ s $^{-1}$

REFERENCES

Bazzano A. et al. 1998, IAU Circ. n.6873

Boella G., Butler R. C., Perola G. C., Piro L., Scarsi L. & Bleeker J. A. M. 1997a, A&AS 122, 299

Boella G., Chiappetti L., Conti G., Cusumano G., Del Sordo S., La Rosa G., Maccarone M. C., Mineo T., Molendi S., Re S., Sacco B. & Tripiciano M. 1997b, A&AS 122, 327

Bouchet L., et al. 1991, ApJ 338, L45

Branduardi G., Ives J. C., Sandford P. W., Brinkman A. C. & Maraschi L. 1976, MNRAS 175, 47

Chiappetti L., Cusumano G., Del Sordo S., Maccarone M.C., Mineo T. & Molendi S., 1998, in “The Active X-ray Sky - Results from *BeppeSAX* and RXTE”, Nuclear Physics B (Proc. Suppl.) 69/1-3, 610.

Cremonesi D.I., Mereghetti S., Sidoli L. & Israel G.L. 1999, A&A in press

Davies R.D., Walsh D., Browne I. W. A., Edwards M. R. & Noble R. G. 1976, Nature 261, 476

Eyles C.J., Skinner G. K., Willmore A. P., Rosenberg F. D. 1975, Nature 257, 291

Fender R.P. & Stappers B.W. 1998, IAU Circ. 6937

Fiore F., Guainazzi M., Grandi P. 1999, Technical Report v1.2, BeppoSAX Scientific Data Center, available online at <ftp://www.sdc.asi.it/pub/sax/doc/softwaredocs/saxabcv1.2.ps>

Frontera F., Costa E.; Dal Fiume D., Feroci M., Nicastro, L., Orlandini M., Palazzi E. & Zavattini G. 1997, A&AS 122, 357

Goldwurm A., Cordier B., Paul J., Ballet J., Bouchet L., Roques J.P., Vedrenne G., Mandrou, P., Sunyaev, R., Churazov E., Gilfanov M., Finogenov A., Vikhlinin A., Dyachkov A., Khavenson N. & Kovtunenko V. 1994, *Nature* 371, 589

Guainazzi M. & Matteuzzi A. 1997, Technical Report TR-11, BeppoSAX Scientific Data Center, available online at <ftp://www.sdc.asi.it/pub/sax/doc/reports/sdc-tr14.ps>

Grebenev S.A., Pavlinsky M. N., Sunyaev R. 1996, Proc. “Rontgenstrahlung from the Universe”, eds. Zimmermann H.U., Trumper J. and Yorke H., MPE Report 263, p. 141

Helfand D.J. & Becker R.H. 1985, *Nature* 313, 118

Helfand D.J. & Becker R.H. 1987, *ApJ* 314, 203

Hjellming R.M., Rupen M.P., Chigo F., Waltman E.B., Mioduszewski A.J. 1998, *IAU Circ.* 6937

Kawai N., Fenimore E. E., Middleditch J., Cruddace R. G., Fritz G. G., Snyder W. A. & Ulmer M. P. 1988, *ApJ* 330, 130

Kennea J.A. & Skinner G.K., 1996, *PASJ* 48, 117

Koyama K., Maeda Y., Sonobe T., Takeshima T., Tanaka Y. & Yamauchi S. 1996, *PASJ* 48, 249

Lewin W.H.G.; Rutledge R.E., Kommers J.M. Van Paradijs J. & Kouveliotou C. 1996 , *ApJ* 462, L39

Maeda Y. & Koyama K., in “The Galactic Center”, *ASP Conf. Ser.* 102, Ed. R. Gredel, p.423, 1996

Maeda Y., Koyama K., Sakano M., Takeshima T. & Yamauchi S. 1996, *PASJ* 48, 417

Maeda Y. et al. 1998, in “The Central Parsecs”, Galactic Center Workshop 1998, Tucson 1998, Eds. H. Falcke, A. Cotera, W. Huschl, F. Melia, and M. Rieke, in press

Mahadevan R. et al. 1998, in “The Central Parsecs”, Galactic Center Workshop 1998, Tucson 1998, Eds. H. Falcke, A. Cotera, W. Huschl, F. Melia, and M. Rieke, in press

Mayer–Hasselwander H.A. et al. 1998, A&A 335, 161

Melia F. 1992, ApJ 387, L25

Melia F., Fatuzzo M., Yusef-Zadeh F. & Markoff S. 1998, ApJ 508, L65

Menten K.M., Reid M.J., Eckart A. & Genzel R. 1997, ApJ 475, L111

Mereghetti S., Sidoli L. & Israel G.L. 1998, A&A 336, L81

Mewe R., Gronenschild E.H.B.M. & van den Oord, G.H.J. 1985, A&AS 62, 197

Mirabel I.F., Rodriguez L.F., Cordier B., Paul J. & Lebrun F. 1992, Nature 358, 215

Narayan R., Yi I. & Mahadevan R. 1995, Nature, 374, 623

Narayan R., Mahadevan R., Grindlay J.E., Popham R.G., Gammie C. 1998, ApJ 492, 554

Parmar A.N., Martin D.D.E., Baudaz M., Favata F., Kuulkers E., Vacanti G., Lammers U., Peacock A. & Taylor B.G. 1997, A&AS 122, 309

Pavlinsky M.N., Grebenev S.A., & Sunyaev R.A. 1994, ApJ 425, 110

Predehl P. & Trumper J. 1994, A&A 290, L29

Predehl P. et al. 1995, in “Nuclei of Normal Galaxies”, Kluwer, (NATO ASI Series)

Predehl P. & Kulkarni S.R. 1995, A&A 294, L29

Proctor R.J., Skinner G.K. & Willmore A.P. 1978, MNRAS 185, 745

Sakano M., Imanishi K., Tsujimoto M., Koyama K., & Maeda Y., 1999, ApJ 520, in press

Shaver P.A., Salter C.J., Patnaik A.R., Van Gorkom J.H., Hunt G.C. 1985, Nature 313, 113

Sidoli L., Israel G.L., Chiappetti L., Treves A., Orlandini M., Kuulkers E., Predehl P., Heise J. & Mereghetti S., 1998a, in “The Active X-ray Sky - Results from *BeppoSAX* and RXTE”, Nuclear Physics B (Proc.Suppl.) 69/1-3, 88.

Sidoli L., Mereghetti S., Israel G.L., Cusumano G., Chiappetti L. & Treves A. 1998b, A&A 336, L81.

Sidoli L., Mereghetti S., Chiappetti L., Heise J., Israel G.L., Kuulkers E., Orlandini M., Predehl P., Tiengo A. & Treves A. 1999, proc. Third INTEGRAL Workshop, “The Extreme Universe”, Taormina 1998, in press

Smith D.A., Levine A. & Wood A. 1998, IAU Circ. n.6932

Skinner G.K., Willmore A.P., Eyles C.J., Bertram D., Church M.J., Harper P.K.S, Herring J.R.H., Peden J.C.M., Pollock A.M.T., Ponman T.J. & Watt M.P. 1987, Nature 330, 544

Skinner G.K., Foster A.J., Willmore A.P., Eyles C.J. 1990, MNRAS 243, 72

Skinner G.K. 1993, A&ASS 97,149

Strohmayer T. & Marshall F.E. 1998, IAU Circ. n.6934

Sunyaev R.A. & Titarchuk L.G. 1980, A&A 86, 121

Sunyaev R.A., Churazov E., Gilfanov M., Pavlinsky M., Grebenev S., Babalyan G., Dekhanov I., Yamburenko N., Bouchet L., Niel M., Roques J.P., Mandrou P., Goldwurm A., Cordier B., Laurent PH., Paul J. 1991a, A&A 247, L29

Sunyaev R.A. et al. 1991b, *Adv. Space Res.* 11, 177

Ubertini P. et al. 1999, proc. Third INTEGRAL Workshop, “The Extreme Universe”,
Taormina 1998, in press

van Paradijs J. 1995, in *X-ray Binaries*, eds. W.H.Lewin, J.P.E. van den Heuvel & J. Van
Paradijs, Cambridge University Press, p. 536

Watson M.G., Willingale R., Grindlay J.E. & Hertz P. 1981, *ApJ* 250, 142

Wijnands R. & van der Klis M. 1998, *Nature*, 394, 344

Yusef-Zadeh F. & Bally J. 1987, *Nature* 330, 455

Yusef-Zadeh F., Purcell W. & Gotthelf E. 1997, Proc. 4th Compton Symp., p.1027

in't Zand J.J. et al. 1990, *Adv. Space Res.* 11, 187

in't Zand J.J. et al. 1998a, *A&A* 331, L25

in't Zand J.J. et al. 1998b, IAU circ. n.6846

in't Zand J.J. et al. 1998c, IAU circ. n.6840

Fig. 1.— Mosaic of the Galactic Center region images obtained with the MECS3 instrument in the 2–10 keV energy range. North is to the top, East to the left. Coordinates are for the J2000 equinox. The image has been corrected for the vignetting and for the differences in the relative exposure lengths of the various observations.

Fig. 2.— Positions of the X-ray sources in the vicinity of SgrA* superimposed on the MECS 2–10 keV image. The error circles have radii of $20''$ for the ROSAT sources (PT, from Predehl & Trumper 1994), $1'$ for AX J1745.6–2901 (Maeda et al. 1996) and $1'$ for 1E 1742.5–2859 (Watson et al. 1981). The two crosses mark the accurate positions, obtained with radio observations, of SgrA* ($R.A. = 17h\ 45m\ 40.131s$, $Dec. = -29^\circ\ 00' 27.5''$, Menten et al. (1997)) and A 1742–289 (Davies et al. 1976). The large circle ($2'$ radius) corresponds to the extraction region of the counts used in the spectral analysis. All the coordinates are for the J2000 equinox.

Fig. 3.— Radial profile of the X-ray emission from the GC region in the 2–5 keV range (upper panel) and in the 5–10 keV range (lower panel). The data points represent the surface brightness measured in concentric rings centered at the position of SgrA*, while the solid lines show for comparison the profiles expected in the case of a single unresolved point source. Both curves are background subtracted. The expected profiles have been normalized to yield the same number of counts within $10'$ as the measured data. Independently of the relative normalization, the different slope of the two profiles demonstrates that a single point source at the GC cannot account for all the observed emission.

Fig. 4.— Spectrum of the X-ray emission within $2'$ of SgrA* fitted with a thermal plasma model with $kT=4$ keV (both MECS). The residuals at energies around ~ 2.4 keV suggest the presence of a multitemperature plasma.

Fig. 5.— Images of the SgrA* region obtained with a single MECS unit (M3). The top and

bottom panels correspond respectively to the soft (2–6 keV) and hard (6–10 keV) energy range.

Fig. 6.— Spectrum of the black hole candidate 1E 1740.7-2942 fitted with a cut-off power law (see Table 3 for the parameters).

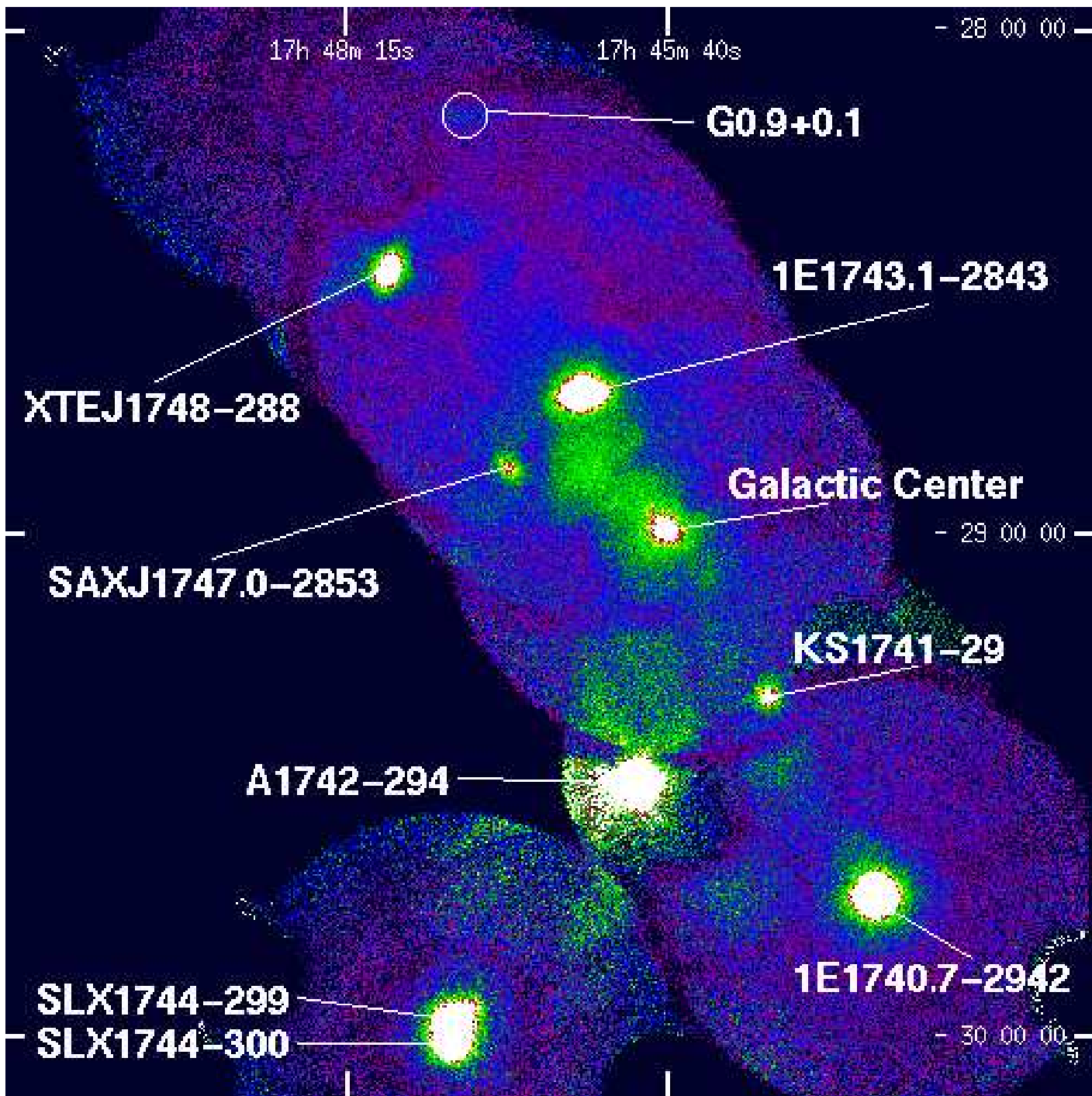
Fig. 7.— Background subtracted light curves of A 1742-294, binned in 5000 s long time intervals.

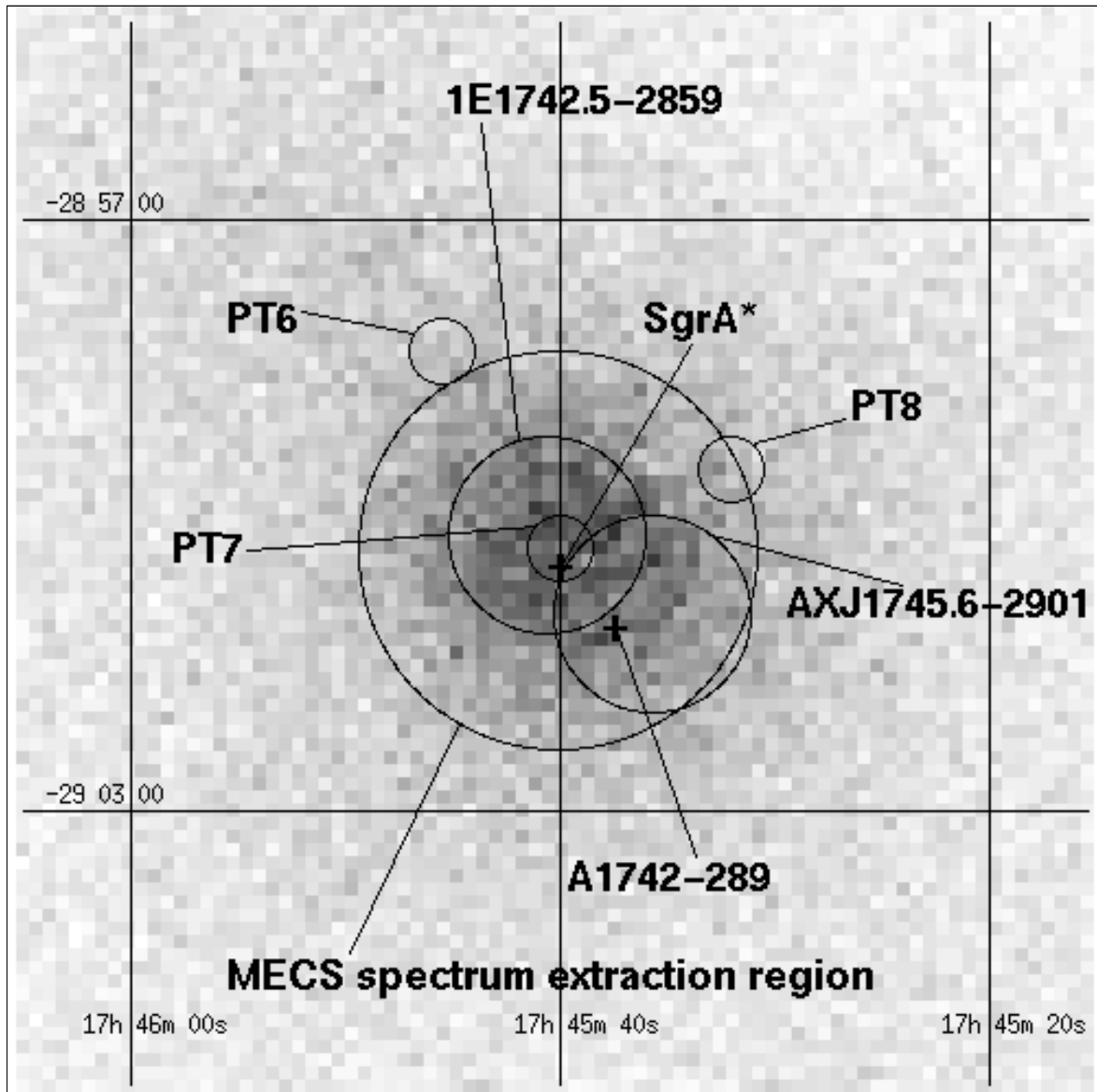
Fig. 8.— Detail of the 1998 outburst of XTE J1748-288 as observed by the XTE ASM. The ASM detections at more than 3 sigma are plotted as error bars, while the remaining ASM points are shown as diamonds. The vertical dashed lines indicate the epochs of start and end of our observation (n. 11), while the horizontal dashed line indicates the flux level measured by BeppoSAX. Note that the BeppoSAX flux measurement represents a significant detection of XTE J1748-288 at a level well below the ASM sensitivity threshold and consistent with an extrapolation of the ASM light curve.

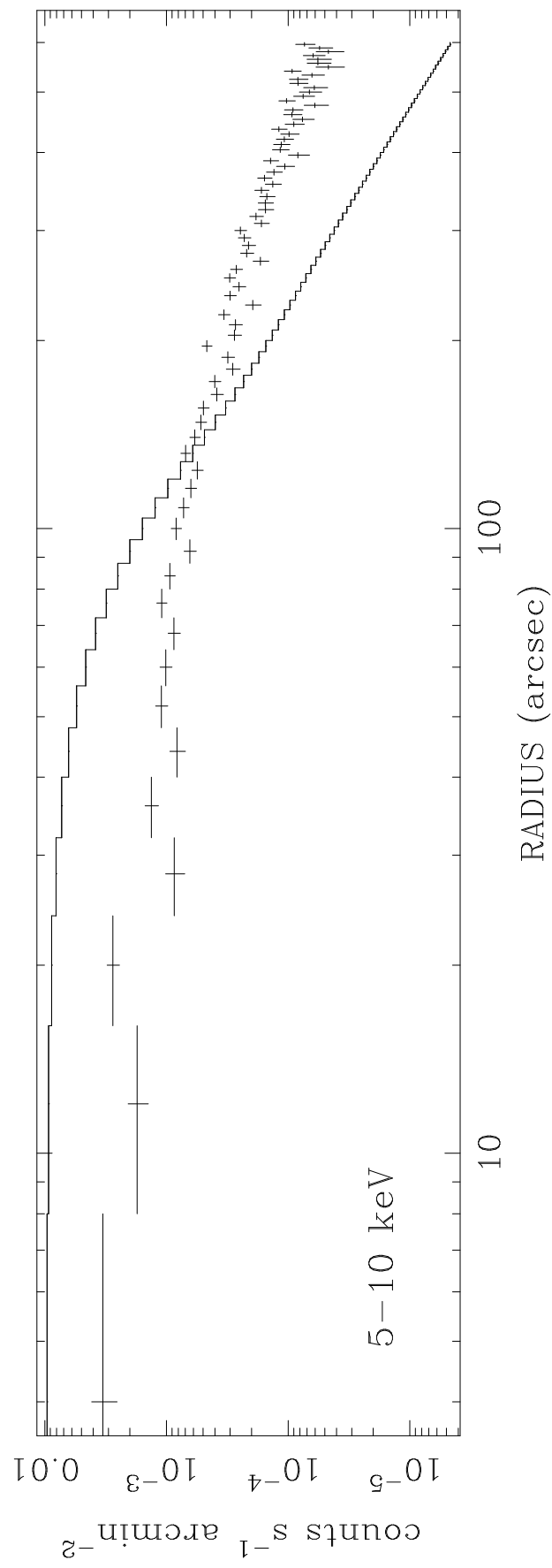
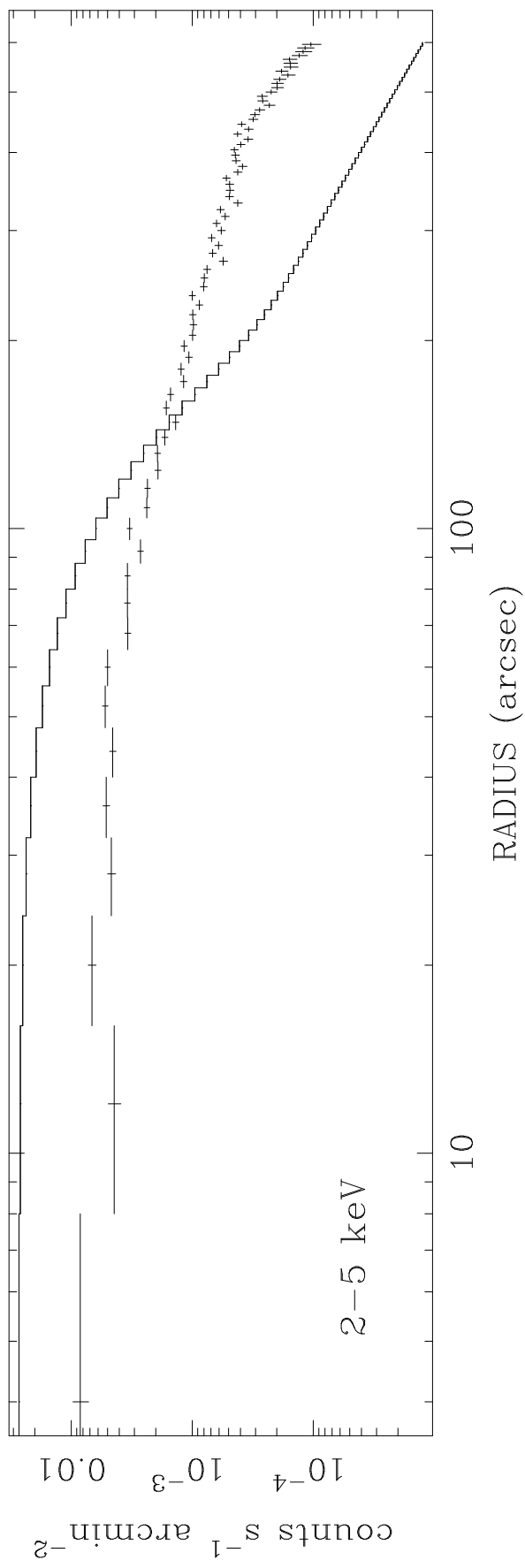
Fig. 9.— Left panel: light curve of the burst from SAX J1747.0–2853 in different energy ranges. The dotted and dashed lines indicate the level of the persistent emission in the contiguous time interval respectively before and after the burst. The burst is well detected also in the PDS instrument above \sim 12 keV. Right panel: Results obtained by fitting the burst emission in different time intervals with a blackbody model.

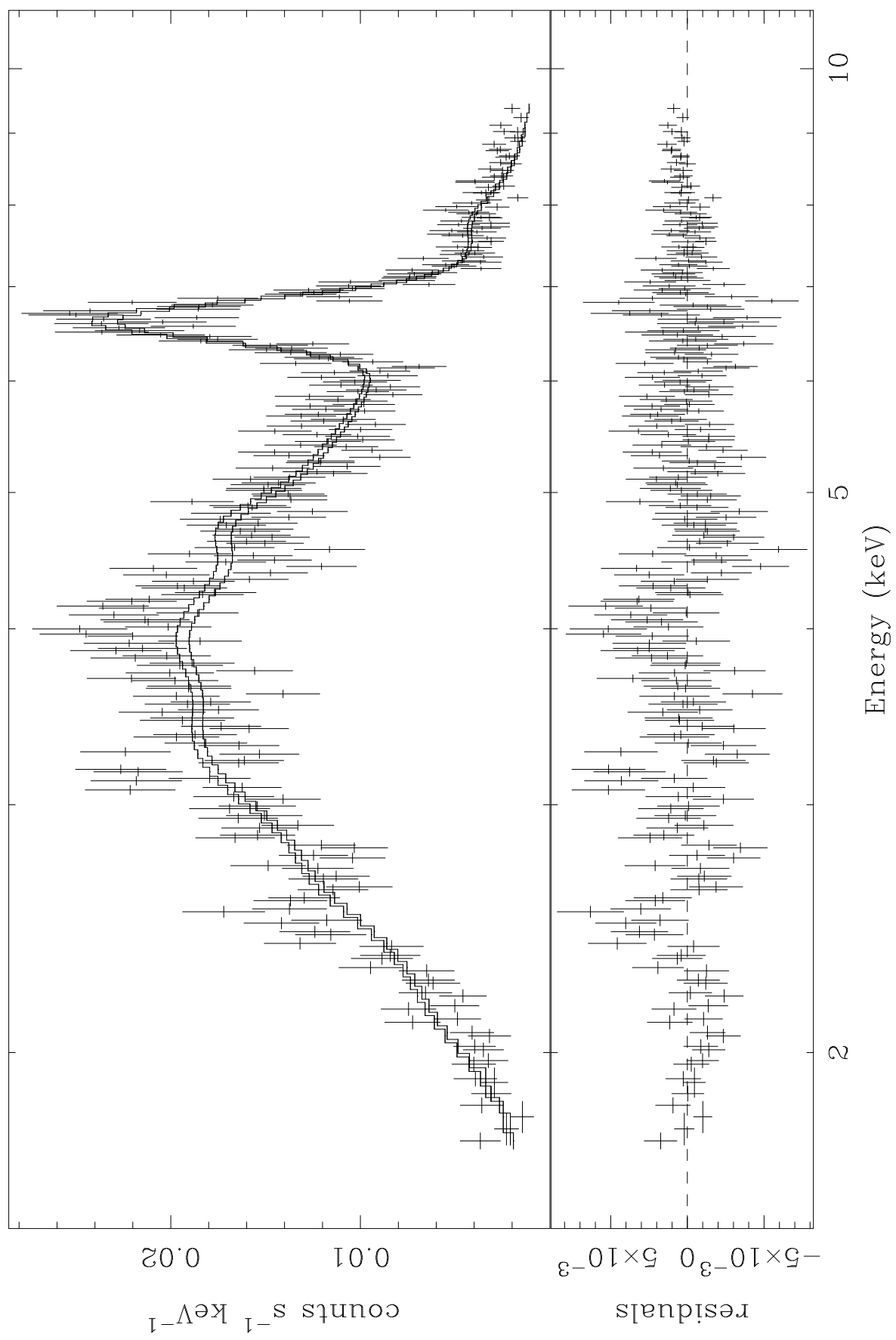
Fig. 10.— MECS Image (M3 unit) of the region containing SLX 1744–299, SLX 1744–300 and the “Mouse” in the 6–10 keV energy range.

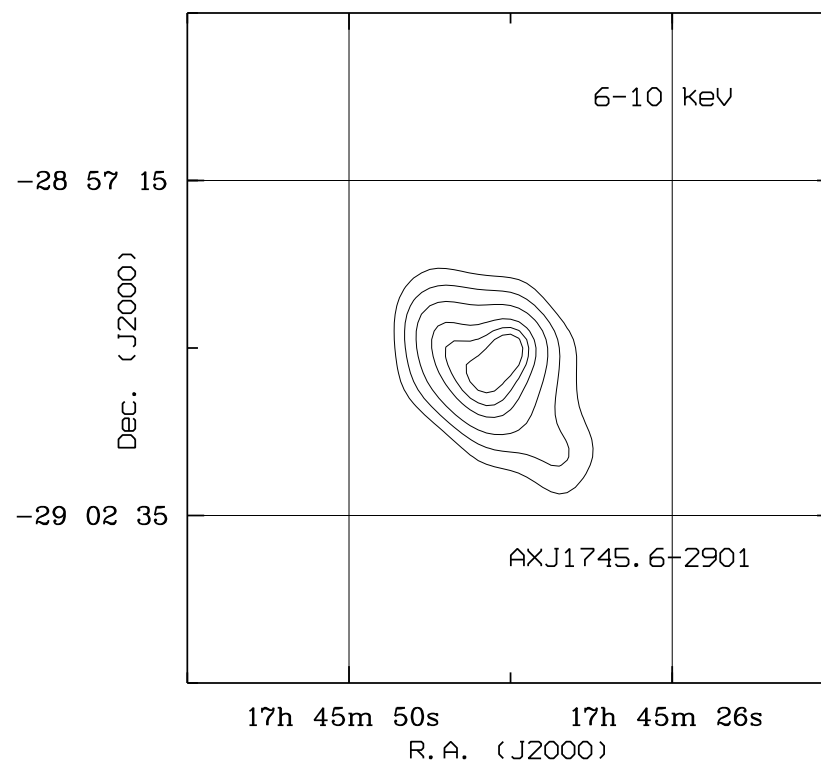
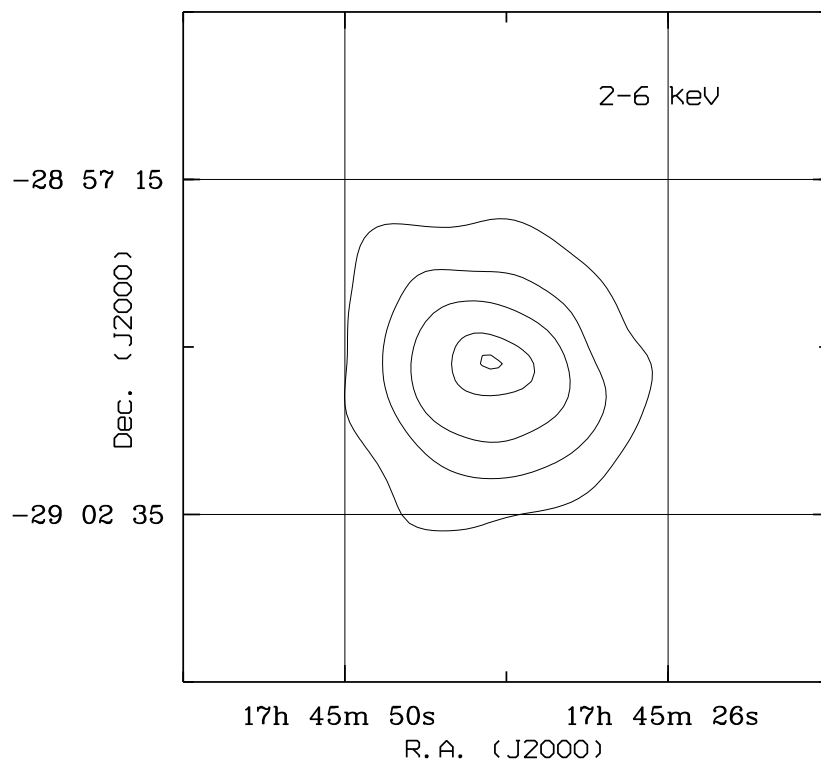
Fig. 11.— Absorbing column density and 2–10 keV spectral slope (power law photon index) for the sources in the GC region. The triangles mark the black hole candidates, while sources that showed Type I X-ray bursts are indicated with squares.

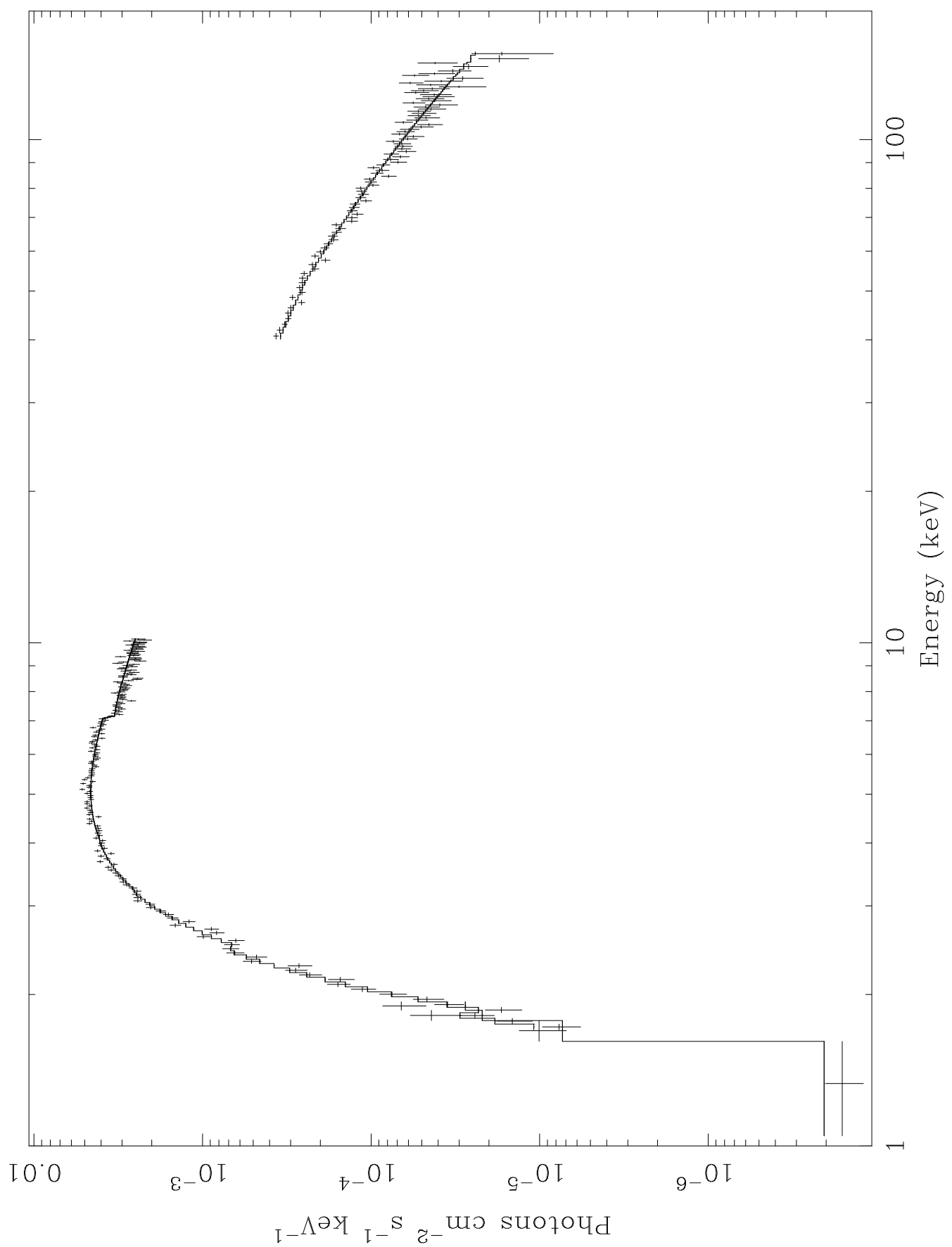


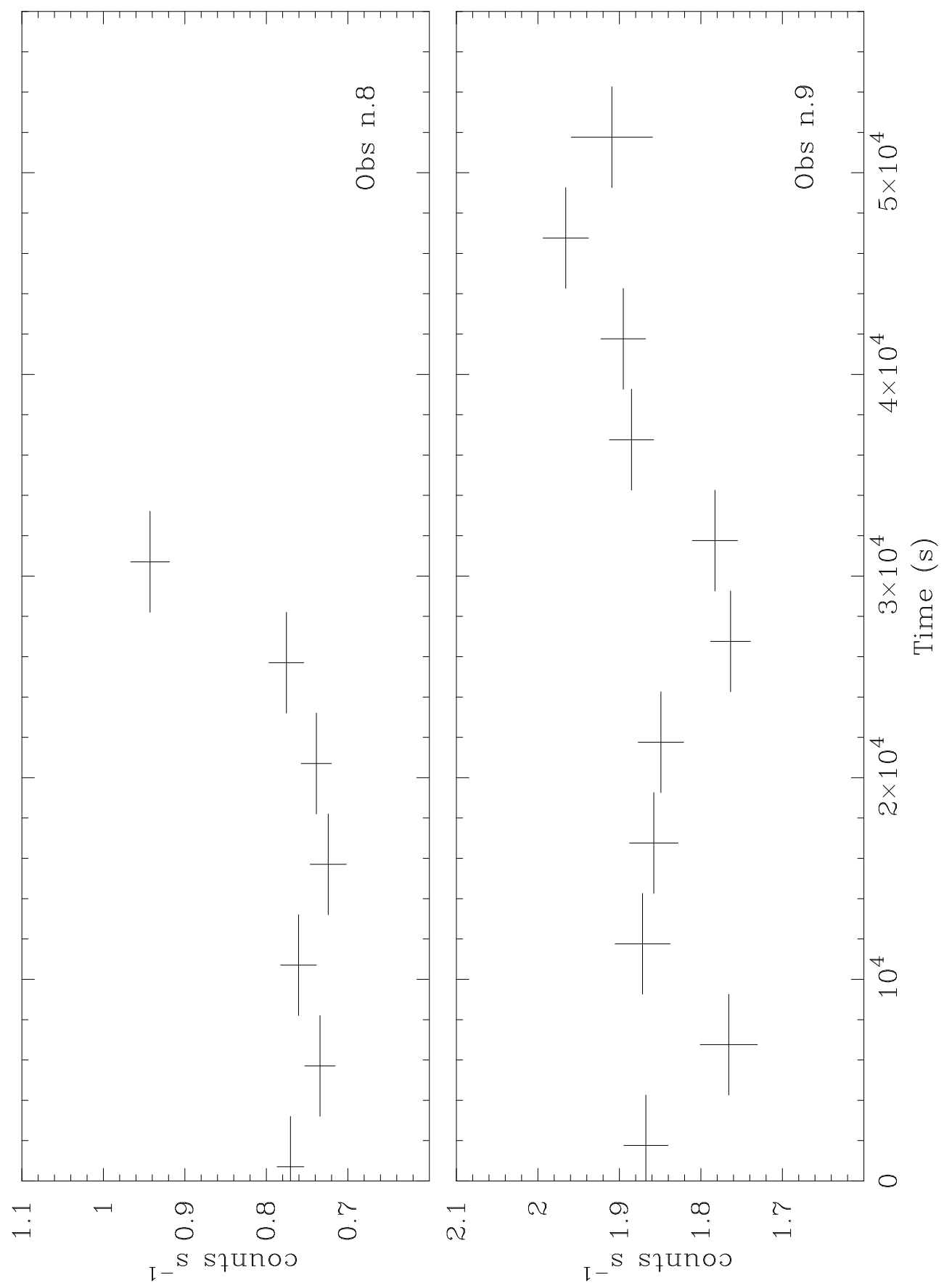




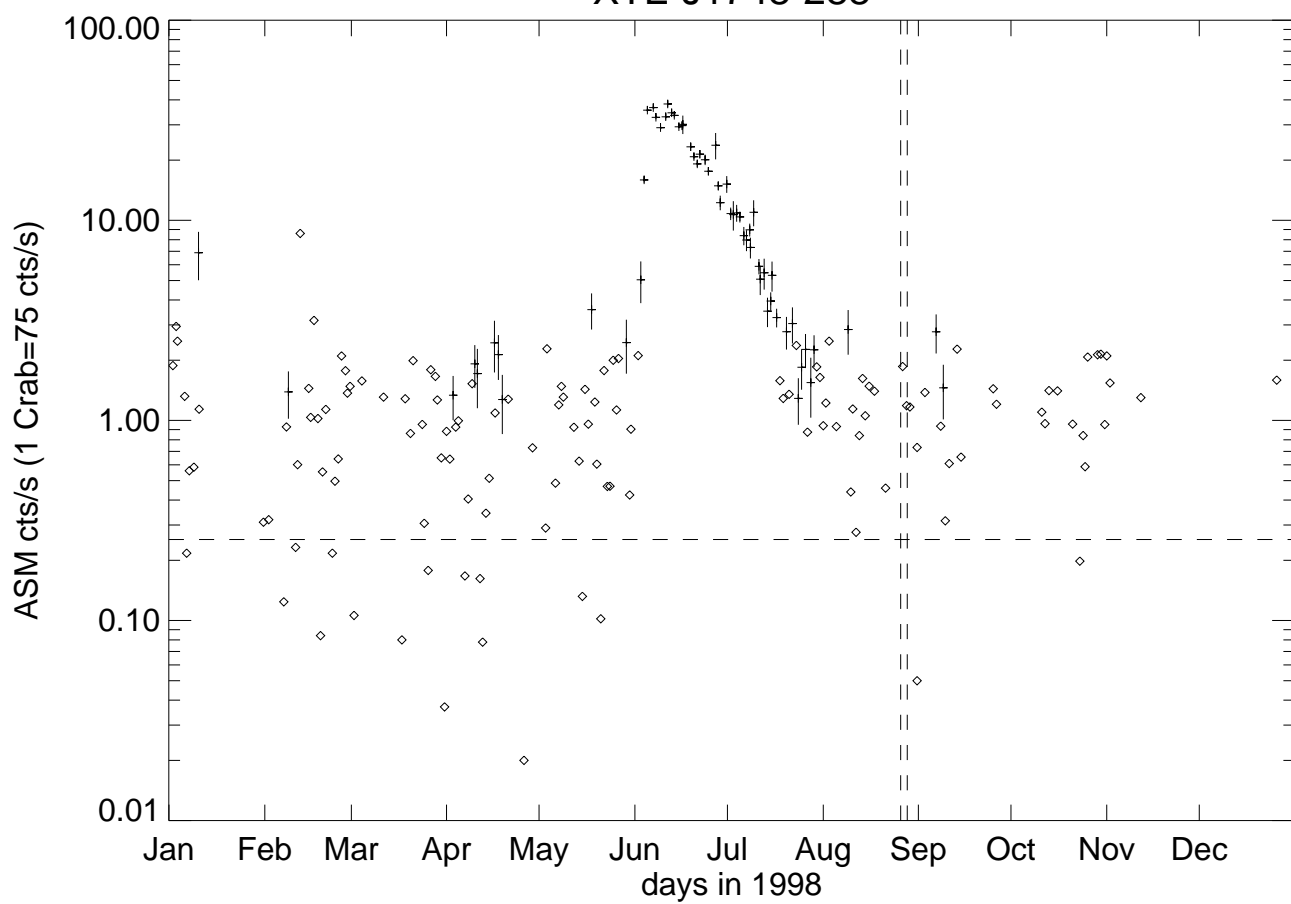


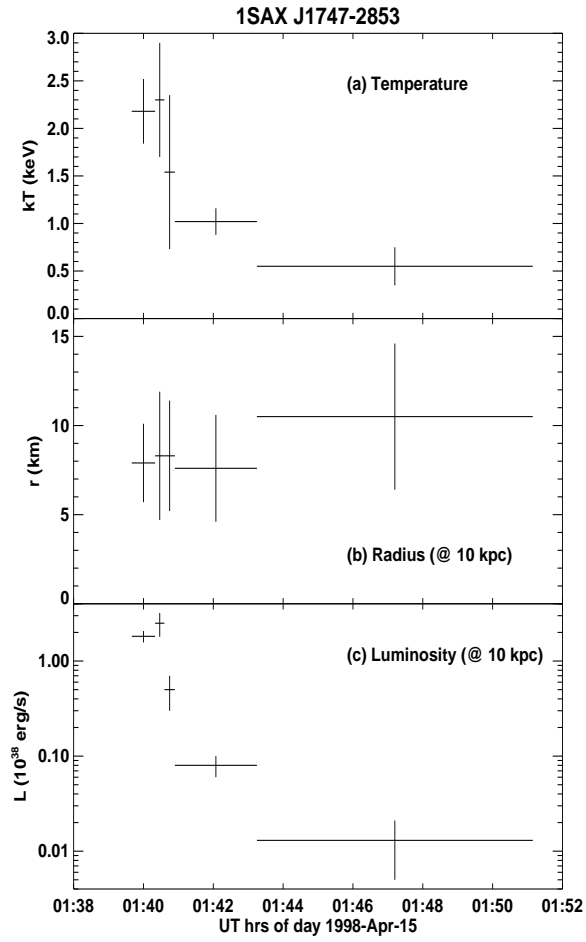
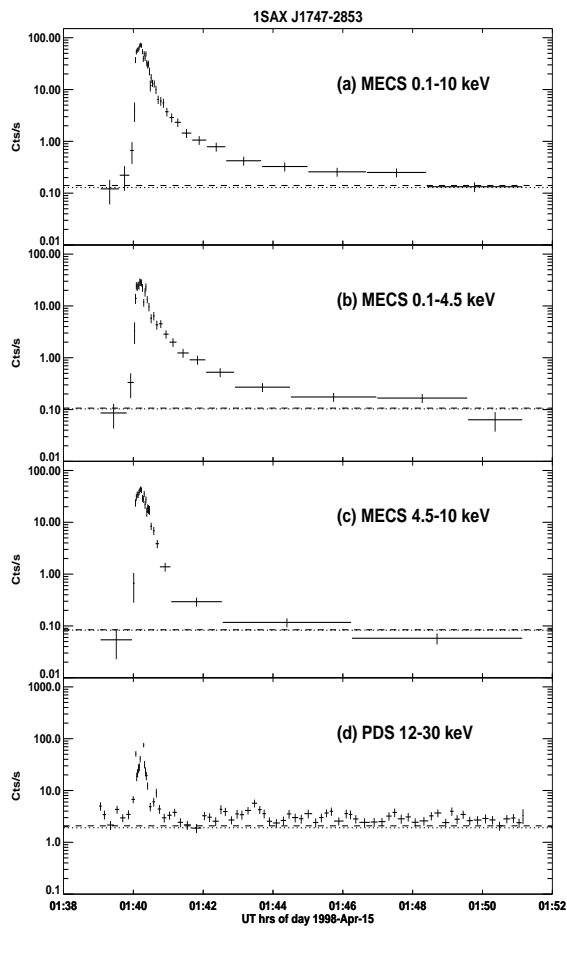


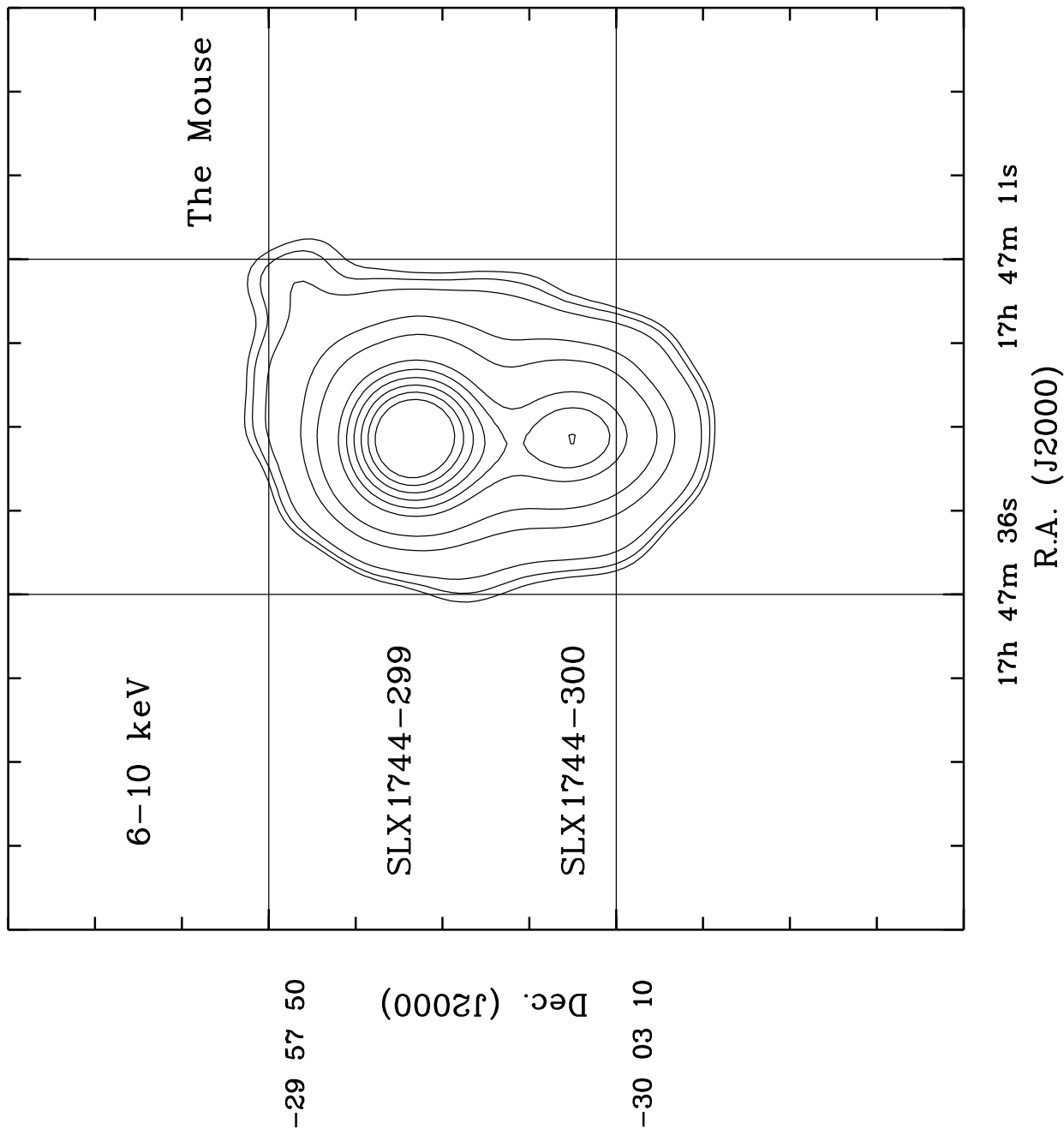


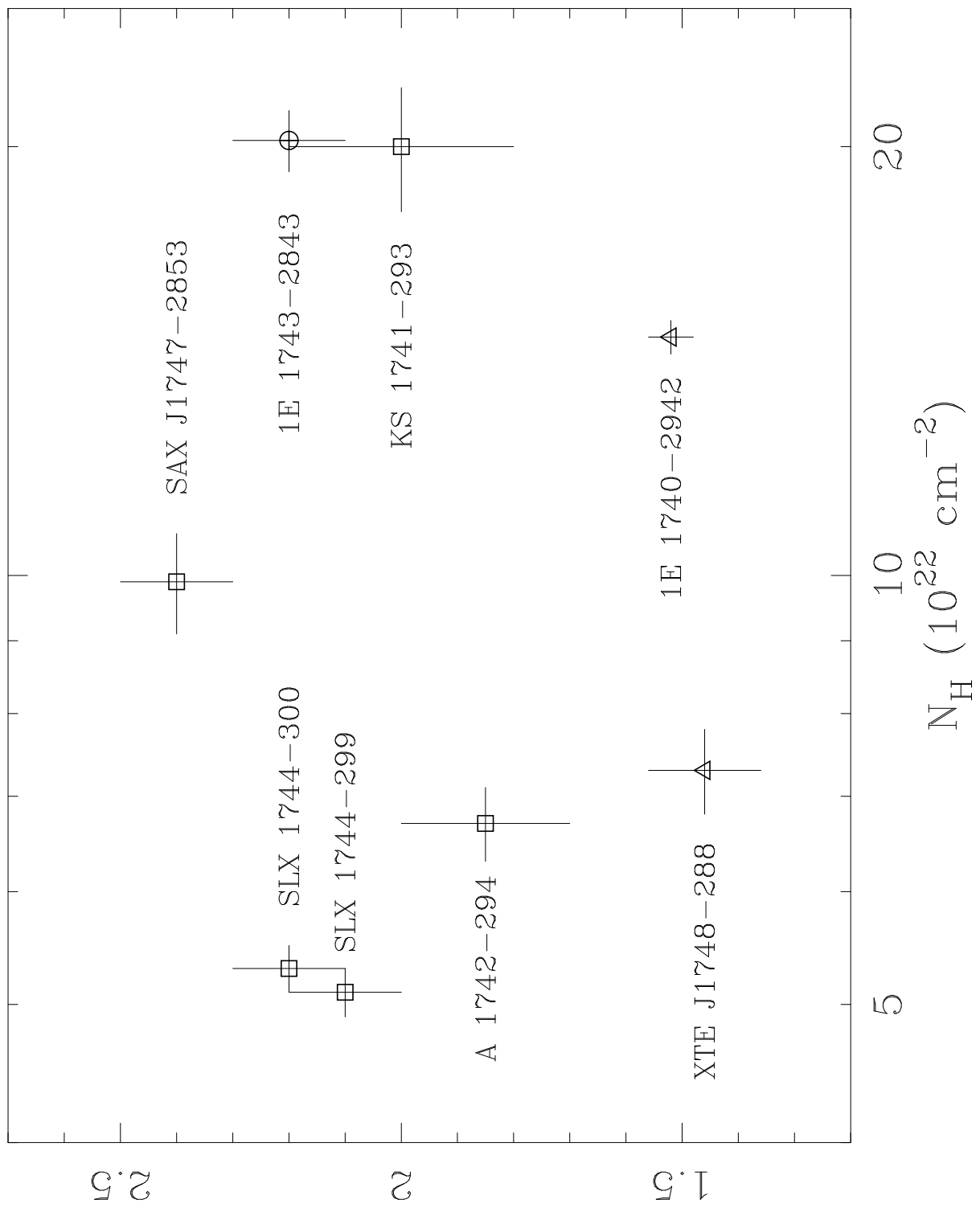


XTE J1748-288









POWER LAW PHOTON INDEX